Materials Science-Poland, 37(2), 2019, pp. 265-279
http://www.materialsscience.pwr.wroc.pl/
DOI: 10.2478/msp-2019-0028

sciendo

Selective crystallization of gamma glycine for NLO applications using magnesium sulfate ($MgSO_4$) as an additive

S. Anbu Chudar Azhagan*, V.S. Kathiravan

Department of Physics, Govt.College of Technology, Coimbatore-641013, India

Crystallization of γ-glycine in the presence of selected concentration (9 g/mL) of tailor-made additive magnesium sulfate heptahydrate salt ($MgSO_4 \cdot 7H_2O$) has been studied at ambient temperature by adopting slow solvent evaporation procedure. The morphological modifications of glycine crystals grown from pure aqueous solutions of glycine and from glycine solutions containing magnesium species in the amount of 0.1 g/mL to 16 g/mL have been investigated thoroughly. The crystalline nature and phase identification of the crystalline material were confirmed by X-ray powder diffraction and SXRD studies. NMR studies revealed the information about the molecular conformation in solution, phase changes, functional groups and chemical environment. FT-IR spectra revealed distinct difference between α and γ-glycine polymorphs in the region around 880 cm^{-1} to 930 cm^{-1}. The grown γ-glycine crystal had a lower cut-off value at 200 nm and the bandgap value evaluated from the Tauc plot was found to be 5.83 eV. The marked differences between α and γ-polymorphs of glycine were also revealed by DSC thermograms. The mechanical strength of the γ-glycine crystal was studied with the help of Vickers microhardness instrument. Kurtz-powder NLO study proved the generation of second harmonics (i.e. green light emission) in the grown γ-glycine crystal and its efficiency was calculated as 1.44 times better than that of the reference material potassium dihydrogen phosphate.

Keywords: *X-ray diffraction; solvents; single crystal growth; nucleation; solubility; crystal morphology*

1. Introduction

New nonlinear optical materials are necessary to meet the requirements of day to day technological applications. Among the twenty protein aminoacids, the simplest one is glycine (NH_2CH_2COOH) existing as zwitterion both in aqueous solution and in the solid state. Three different polymorphic forms, such as metastable α-form, unstable β-form and γ-form stable at ambient temperature were reported for glycine. The building blocks of α-glycine are cyclic dimers, while the building blocks of γ-glycine, are helical dimers. The combination of dipole-dipole and hydrogen-bonding forces results in both types of dimers. The order of thermodynamic stability of glycine polymorphs was found to be $\gamma > \alpha > \beta$. The crystal structure of γ-glycine consists of zwitterionic glycine molecules aligned in trigonal hemihedral symmetry, three molecules per unit cell. It crystallizes in trigonal–hexagonal crystal system and has a non-centrosymmetric space group $P3_2$ suitable for nonlinear optical, piezoelectric, photonic and pyroelectric applications. The structure of α-glycine crystal consists of zwitterionic glycine molecules aligned end to end, with the second layer antiparallel to the first layer and four molecules per unit cell. It crystallizes in monoclinic crystal system and has a $P2_1/n$ centrosymmetric space group ruling out the possibility of second harmonic generation. The γ-glycine in solid state exists as a dipolar ion. This is due to donation of proton from the carboxylic acid group to the amino group. The resulting chemical structure $NH_3^+CH_2\ COO^-$ consists of carboxylate ion COO^- group and ammonium ion NH_3^+ group. Due to its zwitterionic structure, glycine possesses a high melting point and peculiar physical and chemical properties. Besides, the chromophores present in glycine, such as amino and carboxyl groups, make the crystal more transparent in the UV-Vis-NIR region. Challenging polymorph β-glycine is highly unstable and undergoes solution-mediated phase transformation in solution, thereby

*E-mail: anbuchudarazhagan@gmail.com

it transforms rapidly into other forms of glycine. From the thorough literature study of glycine polymorphs it was concluded that metastable α-polymorphic form of glycine produces spontaneously in pure aqueous solutions whereas the most thermodynamically stable form γ-glycine can be obtained in acidic or basic solution, low pH or high pH solutions or in the presence of inorganic salts or tailor made additives [1–16, 19–22]. In recent times, γ-glycine single crystals have grown in the presence of potassium chloride [31], magnesium chloride [15], phosphoric acid [16], ammonium acetate [17], ammonium carbonate [18], zinc acetate [23], strontium chloride [29], cesium chloride [30] and ammonia solutions [24]. In the present research article, we report the growth and characterization of γ-glycine crystal grown from a mixture of water and magnesium sulfate solvent by slow solvent evaporation procedure. The harvested glycine crystals were subjected to characterization studies, namely X-ray powder diffraction, single crystal X-ray diffraction, proton ^{1}H and carbon ^{13}C NMR spectra analysis, spectroscopic FT-IR, elemental ICP-OES, optical UV-Vis-NIR, thermal TG-DTA, DSC, microhardness and SHG to explain the differences in α- and γ-polymorphs of glycine.

2. Experimental

The α- and γ-polymorphs of glycine single crystals were synthesized from a calculated amount of glycine salt (Qualigens AR grade, 99.9 % purity) and selected concentrations (1 g/100 mL and 3 g/100 mL double distilled water) of magnesium sulfate heptahydrate salt (Merck AR grade, 99.9 % purity), chosen from the solubility profile curve. The solubility of glycine polymorphs was measured for various concentrations of magnesium sulfate (1 g/mL to 10 g/mL raised in steps of 1 g/mL). The solubility of γ-glycine increases faster with the increase in concentration of magnesium sulfate, whereas the α-glycine solubility value is a bit lower than that of γ-glycine. The slope of the curve of glycine polymorphs solubility graph is positive as shown in Fig. 1 and it facilitates the crystal growth by slow solvent evaporation procedure. The pH value of the saturated glycine solutions containing 1 g/mL and 3 g/mL magnesium sulfate concentration was measured as pH = 6.2 and 5.72, respectively. The saturated glycine solutions were stirred at a rate of 380 rpm using Remi make magnetic stirrer. The resulting glycine saturated solutions in magnesium sulfate environment were covered with pin perforated polythene plastic sheets and placed in a dust free environment. After the nucleation period between 9 and 14 days, the supersaturated glycine solutions in crystallization dishes yielded crystals of distinct morphologies. An α-glycine single crystal grown from pure aqueous solution without additive is presented in Fig. 2 for habit comparison. The gamma glycine crystal harvested from crystallizing dish with 2 g/mL $MgSO_4$ additive is too undersized. The randomly chosen specimen crystals harvested from the crystallization dishes with additive $MgSO_4$ are depicted in Fig. 3 to Fig. 8. The solubility experiment confirms that γ-glycine is more water soluble than α-glycine in $MgSO_4$ solution.

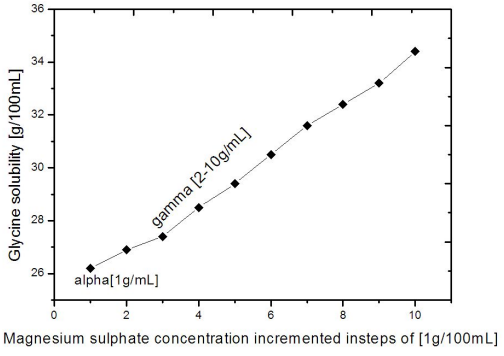

Fig. 1. Glycine polymorphs solubility versus magnesium sulfate concentration.

3. Results and discussion

Li et al. [35] reported that the crystal growth rate is greatly dependent on crystal molecular interactions and solvent-solute interaction in solution. The crystal growth rate is affected by the factors such as level of supersaturation, additive nature and concentration and operating temperature.

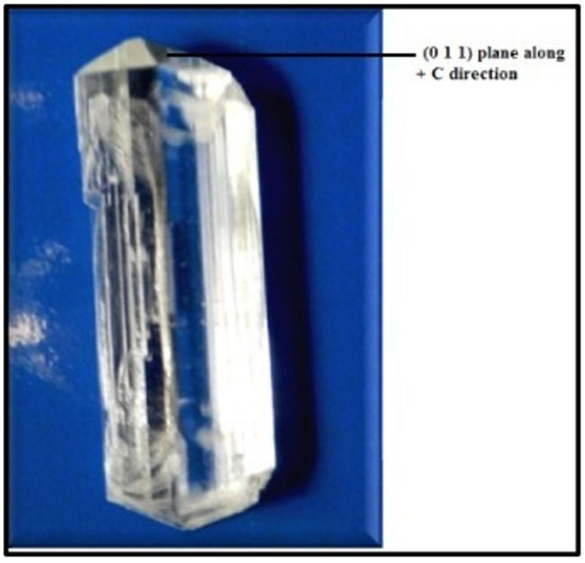

Fig. 2. α-glycine single crystal grown from pure aqueous solution without $MgSO_4$ additive.

Fig. 3. α-glycine single crystals grown from glycine solution with 1g/mL $MgSO_4$ additive.

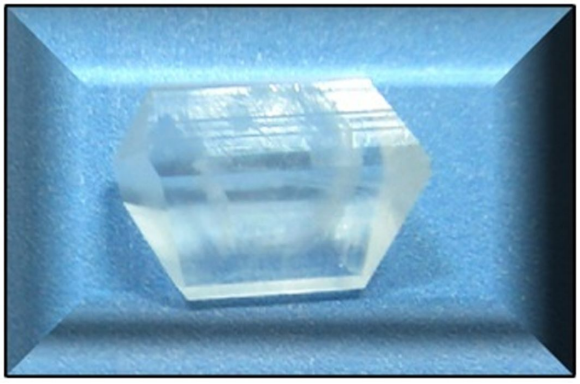

Fig. 4. α-glycine single crystal grown from glycine solution with 1.5 g/mL $MgSO_4$ additive. The crystal is longer in a direction than in c.

Fig. 5. γ-glycine single crystals grown from glycine solution with 3g/mL $MgSO_4$ additive. The crystal is elongated in c-axis direction.

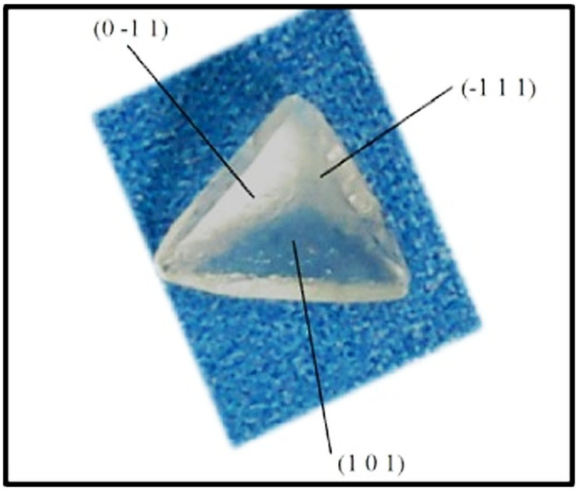

Fig. 6. Indexed crystal morphology of γ-glycine crystal.

The growth rate of a crystal face may be affected by the influence of additives adsorbed on to the crystal growth surface or by changing the properties of solution or interfacial tension caused by crystal/solution and solute molecules aggregated in the solution. The morphology of the crystal may be changed due to anisotropic effects caused by additives which may be adsorbed on a specific crystal face and inhibit its growth. Cabrera et al. [1] have employed the Burton-Cabrera-Frank (BCF) approach of growth mechanism which relates the adsorption of additives and inhibition of growth. If the structure of the host molecule

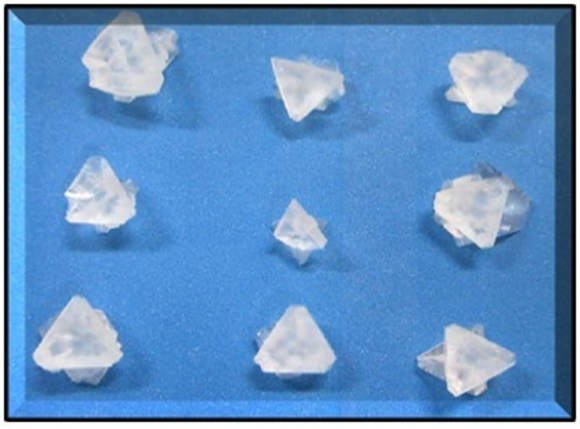

Fig. 7. Twinned trigonal pyramidal shaped γ-glycine single crystals grown from glycine solution with 9 g/mL $MgSO_4$ additive.

Fig. 8. Multiple twinned trigonal pyramidal shaped γ-glycine clusters grown from glycine solution with 16 g/mL $MgSO_4$ additive.

and an additive molecule is similar, then the additive is named as "tailor-made additive". The crystal shape is decided by the relative growth rates of its crystal faces. The favorable adsorption sites are stereo-selected by the presence of tailor-made additive. The adsorption mechanism is classified into two types namely: (i) nucleation kinetics, where interfacial tension between the crystal nuclei and the supersaturated solution may be affected by the impact of adsorption on particular crystal faces; (ii) the additives could hinder the development of critical size of the nuclei by blocking the active growth sites on the embryonic nucleus surface. In certain situations, additives change the solution thermodynamics such as solubility, pH, induction period etc. In the present investigation, the additive magnesium sulfate stereo-selects the favorable adsorption sites in the nucleation of the glycine polymorphs. The growth rate of a crystal face is affected by the influence of magnesium sulfate additive adsorbed on the growing crystal surface and changing the solution properties such as pH and solubility of glycine solution. Moreover, the magnesium sulfate additive influences the solution interfacial tension and aggregation of solute molecules in the solution. The morphology or habit of the glycine crystal grown in magnesium sulfate environment is affected by anisotropic effect. Fig. 2 to Fig. 8 present the crystal photographs of glycine polymorphs. The prismatic bipyramidal crystal habit of large sized α-glycine crystal crystallized spontaneously in supersaturated aqueous solution (Fig. 2). From the photograph (Fig. 2) it is obvious that, (0 1 1) plane is the fast growing crystal face and it is more lengthened along the direction of +c axis than along a-axis. Also, the crystal growth in the opposite direction of c-axis (0 1 $\bar{1}$) takes place at the same rate. The powdered form of this crystal was analyzed by X-ray powder diffraction which confirmed its α-polymorph structure. The introduction of $MgSO_4$ additive into glycine saturated solutions has affected the crystal morphology of the α-glycine appreciably. The typical morphology of α-glycine is obtained in solutions with $MgSO_4$ concentration between 0.1 g/mL and 0.5 g/mL. The α-habit trend alters slightly when the concentration of $MgSO_4$ is increased from 0.5 g/mL to 1.5 g/mL. This morphological modification may be due to selective inhibition of the growth of specific crystal planes by the $MgSO_4$ additive which adsorbs on peculiar sites. As a result, it reduces the growth along c direction as illustrated in Fig. 3 and Fig. 4. This habit trend is continued up to 1.9 g/mL concentration of $MgSO_4$ with even larger reduction in the growth along c-direction. When the critical concentration of $MgSO_4$ is reached ($\geqslant$ 2 g/mL), the resulting crystals get trigonal pyramid shaped smooth facets (unidirectional growth behavior) and truncated tip at one end of the +c-axis (top portion) and rough pyramid shaped non-crystallographic

facets at the opposite end of –c axis (bottom portion), as shown in Fig. 5. Their indexed morphology is depicted in Fig. 6. This type of unidirectional growth was observed in many polar acentric crystals as reported in the literature [33, 34]. Further it was confirmed by single and powder XRD studies that the grown crystal crystallized in γ-polymorph. With further increment in $MgSO_4$ concentration (>8 g/mL), the secondary trigonal pyramid shaped crystal has grown over the top of the truncated tip of the primary crystal due to twinned nucleation, as presented in Fig. 7. At the highest $MgSO_4$ concentration (>15 g/mL), crystal faces got deteriorated which resulted in numerous clusters of γ-glycine crystal overlapped due to multiple twinned nucleation, as depicted in Fig. 8. Srinivasan et al. [25, 26] reported that when the concentration of NaCl in glycine solutions goes beyond a certain level (>12 g/mL) only crystals (i.e. γ-form of glycine) with destructed morphology are produced. Contrary to Srinivasan work, addition of KCl at the concentration up to 18 g/mL into glycine solutions produced good quality γ-glycine crystals with distinct morphology as reported by Sekar et al. [31]. In the present work, addition of $MgSO_4$ up to 8 g/mL into glycine solutions produced good quality γ-glycine crystals with distinct morphology. When the concentration of $MgSO_4$ in glycine solutions was above a certain level (>15 g/mL) γ-form of glycine crystals with destructed morphology was produced.

3.1. Single crystal XRD examination

The grown γ-glycine crystals were subjected to single crystal XRD examination using CAD4-MV31 diffractometer to obtain the unit cell parameters and identify the crystal system. The computed lattice parameters of the grown γ-glycine crystal are a = 7.13 Å, b = 7.13 Å, c = 5.55 Åand $\alpha = \beta = 90°$, $\gamma = 120°$ and cell volume V = 244 $Å^3$. The crystal belongs to hexagonal system and its space group is $P3_2$ which is non-centrosymmetric space group suitable for frequency doubling as well as nonlinear optical and photonics applications.

3.2. Elemental analysis, ICP-OES test

The basic principle behind inductively coupled plasma optical emission spectrometry analysis is that whenever an atom or ion is in an excited state it will return back to the ground state by emitting its characteristic wavelength. The corresponding intensity of the light is proportional to the concentration of that particular element present in the sample solution. This test provides information about qualitative and quantitative data of metals, certain non-metals, and elements in the solution. The test can be employed for determination of presence of Mg element in the grown glycine crystal samples. The required powdered sample was of 10 mg to 20 mg for this study. The powdered glycine sample was transferred into a 25 mL volumetric flask and diluted with deionized water to a required volume. The filtered glycine sample was analyzed with ICP-OES system whose detection limit is 0.01 ppm [15, 29]. The percentage of magnesium element present in the powdered glycine sample prepared at 3 g/100 mL concentration of $MgSO_4$ was found to be 0.04 ppm; γ-polymorph of glycine was later confirmed by SXRD, PXRD, NMR, TG-DTA and DSC studies. Although the additive concentration of $MgSO_4$ in the crystalline matrix was found to be low, but its presence in glycine solutions was significant to grow the γ-polymorph of glycine most favorably. Further it was concluded from the ICP-OES study that the final additive concentration of $MgSO_4$ within the host crystal lattice is not proportional to the concentration used in the process of crystallization since the additive can be incorporated to the host crystal lattice only in a controlled amount.

3.3. X-ray powder diffraction examination

X-ray powder diffraction analysis was made on the finely powdered glycine sample prepared from 1 g/100 mL and 3 g/100 mL concentrations of $MgSO_4$. X-ray powder diffractogram was recorded using Bruker AXS D8 advance X-ray powder diffractometer with CuKα radiation (λ = 1.54060 Å). The finely powdered glycine samples were scanned in the range of 2θ = 10°

to 70° at a scan rate of 1° per minute. The observed peaks in the X-ray powder diffractogram were indexed with hexagonal crystal structure and the unit cell dimensions were calculated using unit cell software program. The recorded X-ray powder diffractogram of both α and γ-glycine polymorphs are depicted in Fig. 9. The unit cell program computed the lattice parameters for the grown γ-glycine crystal to be a = b = 7.057 Å, c = 5.501 Å, α = β = 90°, γ = 120° and unit cell volume V = 237 Å^3. The computed results of XRD powder match well with the reported literature values [28–32]. The dominant or characteristic 100 % peak (2θ) of γ-glycine polymorph is positioned at ≈ 25° and its corresponding h k l plane is (1 1 0) plane. Further, from the X-ray powder diffraction analysis, it was inferred that with increasing $MgSO_4$ concentration, the characteristic 100 % peak and other intense peaks of glycine polymorphs are slightly shifted to lower 2θ angle side as a consequence of a slight increase in the lattice constant. This may be due to the inclusion of trace amount of $MgSO_4$ impurity into the crystal lattice of γ-glycine. The ionic radius of magnesium cation Mg^{2+} is 0.72 Å which is a very small value. Therefore it is predicted that the additive may be introduced into the crystalline matrix as interstitial without disturbing the overall crystal charge neutrality. Moreover, it is found that two Bragg peaks (not indexed) situated at 2θ = 40.8° (5 2 0 plane) and 45.1° (2 2 3 plane) in gamma glycine X-ray powder diffractogram coincide well with pure magnesium sulfate heptahydrate JCPDS Card File No. 36-0419 [32].

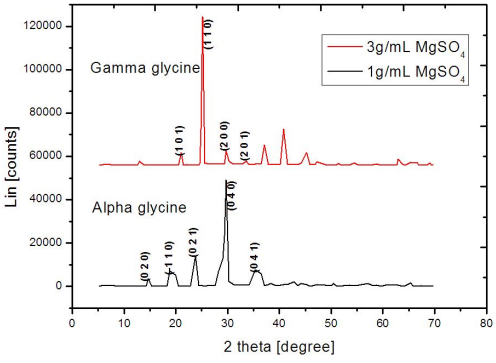

Fig. 9. Indexed X-ray powder diffractogram of α and γ-glycine.

3.4. Chemical nuclear magnetic resonance examination on γ-glycine crystal

Nuclear magnetic resonance spectroscopy is a well-known procedure for characterizing crystalline materials. The structural and dynamic state of functional groups present in molecules can be explored by the application of NMR spectroscopy [37, 38]. The proton ^{1}H and ^{13}C NMR spectra of the grown γ-glycine crystal have been recorded using D_2O as a solvent on a FT NMR spectrometer Bruker Advance III operated at a frequency of 400 MHz at 296 K to confirm the presence of functional groups. The obtained ^{1}H and ^{13}C NMR spectra are depicted in Fig. 10 and Fig. 11, respectively. The chemical shifts δ and their assignments are presented in Table 1. The unit of chemical shift δ is ppm. The disappearance of N–H and COOH groups signals in NMR spectra is due to fast deuterium exchange taking place between the two groups in D_2O solvent. The resonance signal appearing at δ = 3.465 ppm is attributed to methylene group CH_2 protons of γ-glycine molecule whereas the broad signal positioned at δ = 4.684 ppm is attributed to water molecule H_2O in the D_2O solvent. The characteristic ^{13}C NMR spectrum shows two resonance signals at δ = 41.433 ppm and 172.412 ppm, respectively. The resonance signals situated at δ = 41.433 ppm and 172.412 ppm are attributed to methylene group CH_2 and carboxyl carbon group (COO^-), respectively. Anbuchezhiyan et al. [29] reported that the effect of strontium chloride on γ-glycine molecule produced resonance signals δ = 3.3 ppm and 4.633 ppm in proton ^{1}H NMR and δ = 41.35 ppm and 172.37 ppm, respectively, in ^{13}C NMR spectra. In the present NMR investigation, the observed NMR resonance signal chemical shifts are in line with Anbuchezhiyan et al. [29] with a slight increment in chemical shift ppm values (Table 1). This increase in chemical shift values may be due to the presence of magnesium species in the γ-glycine salt. Thus, the above investigation

revealed that the additive $MgSO_4$ shifts the resonance peak slightly to higher ppm side compared to strontium chloride additive as reported by Anbuchezhiyan et al. [29].

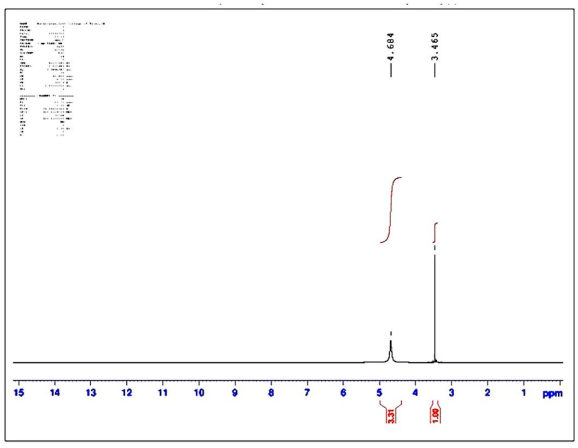

Fig. 10. γ-glycine chemical shift δ assignment in proton ^1H NMR spectrum.

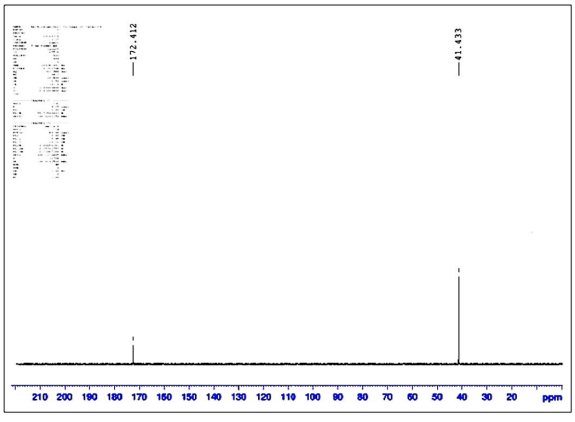

Fig. 11. γ-glycine chemical shift δ assignment in carbon ^{13}C NMR spectrum.

3.5. Spectroscopic FT-IR study on glycine polymorphs

FT-IR is a very valuable tool for identifying chemicals that are either organic or inorganic and presence of polymorphic forms in pharmaceutical chemicals. It can be employed to determine some components of an unknown mixture and for the analysis of solids, liquids, and gases. It is an excellent tool for classifying types of chemical bonds in a molecule by producing an infrared absorption spectrum as a molecular "fingerprint" [37, 38]. The wavelength of absorbed light is characteristic of the chemical bond as shown in the FT-IR spectra (Fig. 12). The fundamental principle of FT-IR is that molecular bonds vibrate at various frequencies depending on the element and the type of bonds. For any given bond, there are several specific frequencies at which it can vibrate. These frequencies correspond to the ground state (lowest frequency) and several excited states (higher frequencies) in accordance with quantum mechanics [38]. The powdered glycine samples were taken in KBr pellet phase and recorded in the range of 400 cm^{-1} to 4000 cm^{-1} by Thermo Nicolet, Avatar 370 Fourier transform infrared spectrometer to explore the presence of functional groups quantitatively. The FT-IR spectra of powdered glycine samples grown in the presence of various concentrations of $MgSO_4$ namely 1 g/mL, 4 g/mL, 5 g/mL, 6 g/mL, and 7 g/mL, respectively, are depicted in Fig. 12. The two polymorphic forms, namely α- and γ-glycine can be unambiguously identified from Fig. 12. The results of FT-IR spectra analysis of glycine polymorphs (α- and γ-glycine) obtained at different concentrations of additive magnesium sulfate are presented in Table 2. The carboxylate group absorption peaks observed at wave numbers 695 cm^{-1}, 606 cm^{-1} and 501 cm^{-1} are attributed to COO^- bending, COO^- wagging and COO^- rocking vibrations, respectively. The ammonium group absorption peaks NH_3^+ observed at wave numbers 3172 cm^{-1}, 2616 cm^{-1}, 1512 cm^{-1} and 1116 cm^{-1} are attributed to NH_3^+ stretching, NH_3^+ group, NH_3^+ rocking mode vibrations, respectively. The complex zwitterionic form of glycine molecule ($NH_3^+CH_2{\cdot}COO^-$) is confirmed by the existence of carboxylate group and the ammonium group in the grown crystal. The IR absorption peaks observed at 896 cm^{-1}, 1408 cm^{-1}, 2893 cm^{-1} are attributed to CCN symmetric stretching mode, COO^- symmetric stretching mode and symmetric stretching of CH_2 group vibrations, respectively. The other IR absorption peaks observed at wave numbers 1028 cm^{-1}, 1326 cm^{-1}, 1611 cm^{-1}, 2121 cm^{-1} are assigned to CCN asymmetric stretching vibration, CH_2 twisting vibration, strong asymmetric

Table 1. NMR spectra analysis of gamma glycine crystal.

NMR spectra	In the presence of magnesium sulfate additive	Assignment of group	In the presence of strontium chloride additive
	Chemical shift δ [ppm]	Presence of functional group	Chemical shift δ [ppm]
Proton ^{1}H NMR	$\delta = 3.465$	$-CH_2$ protons group of γ-glycine molecule	$\delta = 3.3$
	$\delta = 4.684$	H_2O in the D_2O solvent	$\delta = 4.633$
Carbon ^{13}C NMR	$\delta = 41.433$	CH_2 methylene carbon group	$\delta = 41.35$
	$\delta = 172.412$	carboxyl carbon (COO^-) group	$\delta = 172.37$
	Present work		Anbuchezhiyan et al. [29]

CO_2 stretching vibration and combinational bonds, respectively. The singlet IR absorption peak at the wave number 896.51 cm^{-1} (1 g/mL $MgSO_4$ concentration) was modified into doublet peak occurring between wave numbers 927 cm^{-1} and 886 cm^{-1}. From this observation, it can be stated that the fingerprint distinction between α- and γ-forms of glycine polymorphs was clearly explained by FT-IR spectroscopy. The COO^- bending vibration absorption peak at the wave number 695.25 cm^{-1} decreased with increment in the $MgSO_4$ concentration. In contrast, the CCN asymmetric stretching vibration, NH_3^+ rocking mode vibration and combinational bond absorption peaks increased with increment in the $MgSO_4$ concentration. Further, the IR doublet peak occurring between wave numbers 927 cm^{-1} and 886 cm^{-1} confirmed the γ-phase of glycine. The observed IR absorption peaks are in line with the literature [28–31, 37]. The significant concentration effect of $MgSO_4$ additive is clearly depicted in FT-IR spectra.

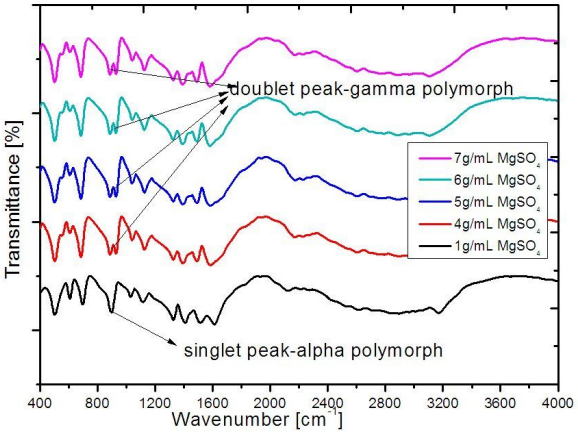

Fig. 12. FT-IR spectra of glycine polymorphs obtained at various concentrations of additive magnesium sulfate.

3.6. Thermal characterization TGA-DTG-DTA thermogram analyses

The results of thermogravimetry (TGA), derivative thermogravimetry (DTG) and differential thermal analysis (DTA) were recorded for γ-glycine sample grown at 3 g/100 mL concentration of $MgSO_4$ to investigate the weight loss, melting point, phase transition temperature and thermal decomposition of the grown crystals. Fig. 13 to Fig. 15 present the traces of TGA, TG-DTG and DTA curves of γ-glycine sample recorded between 38 °C and 750 °C under nitrogen atmosphere at a heating rate of 10°/minute using PerkinElmer Diamond TG/DTA instrument. The initial weight of the γ-glycine sample was about 22.913 mg and the final residue, representing mass decomposition taking place in the sample, was only 6.456 mg. The TGA trace of γ-glycine sample exhibited no weight loss up to 242.24 °C. Since the weight loss occurred beyond 242.24 °C, there was no water of crystallization present in the γ-glycine sample. TGA curve of γ-glycine sample in Fig. 13 shows sudden weight loss starting at 242.24 °C and ending at about 726.5 °C. The major weight loss ($\approx$ 38 %) taking place in the temperature range between 242.24 °C and 288.29 °C could be attributed to the sublimation and decomposition of glycine. The excess weight loss at this temperature range may be due to the release of ammonia NH_3 and CO carbon monoxide molecules. The

Table 2. FT-IR spectra analysis of glycine polymorphs obtained at different concentrations of additive magnesium sulfate.

Concentration of magnesium sulfate in glycine solutions					Vibrational assignments of glycine polymorphs
1 g/mL α-glycine [cm^{-1}]	4 g/mL γ-glycine [cm^{-1}]	5 g/mL γ-glycine [cm^{-1}]	6 g/mL γ-glycine [cm^{-1}]	7 g/mL γ-glycine [cm^{-1}]	
501.11	500.96	500.82	500.80	500.56	–COO– rocking
606.05	605.96	605.86	606.08	606.05	–COO– wagging
695.25	682.83	682.58	682.69	682.58	–COO– bending
896.51	886.33	886.10	886.11	885.99	CCN symmetric stretching vibration
–	926.87	927.05	926.55	926.96	CH_2 rocking
1028.86	1040.08	1040.05	1040.17	1040.04	CCN asymmetric stretching vibration
1116.37	1123.88	1123.62	1123.03	1123.22	NH_3+ rocking mode
1326.77	1326.15	1325.84	1325.40	1325.34	CH_2 twisting
1408.23	1392.42	1391.44	1390.92	1390.50	COO– symmetric stretching
1512.56	1490.43	1490.43	1490.05	1489.96	NH_3+ vibration
1611.39	1582.27	1581.24	1579.68	1579.67	Strong asymmetric CO_2 stretching
2121.83	2172.2	2171.74	2171.63	2171.97	Combinational bond
2616.57	2604.09	2603.3	2602.54	2602.91	NH_3+ stretching vibration
2893.74	–	–	2886.79	2887.87	Symmetric stretching of CH_2 group
3172.67	3107.99	3105.91	3105.49	3106.40	NH_3+ stretching vibration

weight loss between 288.29 °C and 726.5 °C was found to be (≈ 34 %). This weight loss may be attributed to release of $MgSO_4$ from γ-glycine crystal. Derivative-thermogravimetric curve shown in Fig. 14 provides the information pertaining to the change in weight percentage and peak temperature of the sample [36]. As noted in the DTG curve, the weight percentage 99.8 % at about 233.4 °C is due to the loss of water in the sample. The melting starts around 233.4 °C and stops at 271.99 °C with a sharp melting band at about 37.9 °C. The endothermic melting peak temperature is 271.99 °C. To find the possible phase transitions in γ-glycine sample, DTA curve was plotted between heat flow endo up [mW] and temperature [°C]. The DTA trace shown in Fig. 15 reveals the phase transition peak (γ- to α-phase) at 210 °C. Perlovich et al. [36] reported that the phase transition temperature between γ- and α-glycine can range between 165 °C and 201 °C. Thus, in the present work, the phase transition peak is higher than reported by Perlovich et al. [36]. Hence, the grown γ-glycine crystal is more thermodynamically stable material, suitable for laser and NLO applications.

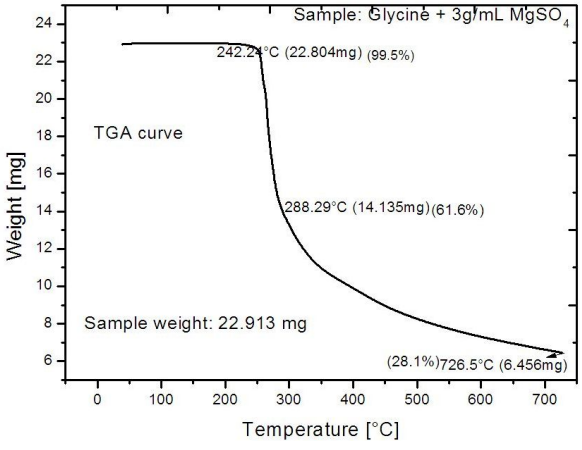

Fig. 13. Thermogravimetric (TGA) curve of γ-glycine crystal.

3.7. Confirmation of phase transition in γ-glycine crystal by thermal DSC studies

Differential scanning calorimetry experiment determines the quantity of heat energy absorbed or released by a sample as it is heated, cooled or held at a constant temperature. The difference in energy input in a substance and a reference

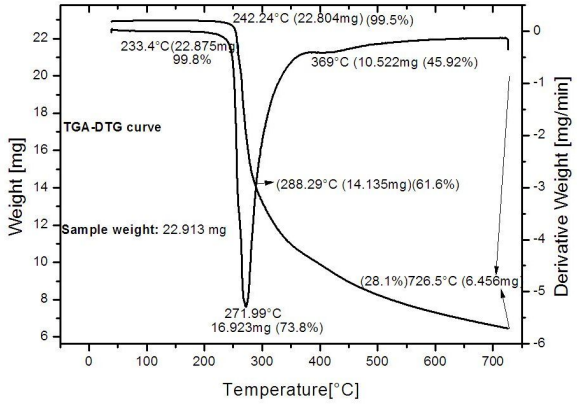

Fig. 14. Thermogravimetric TGA- derivative DTG curve of γ-glycine crystal.

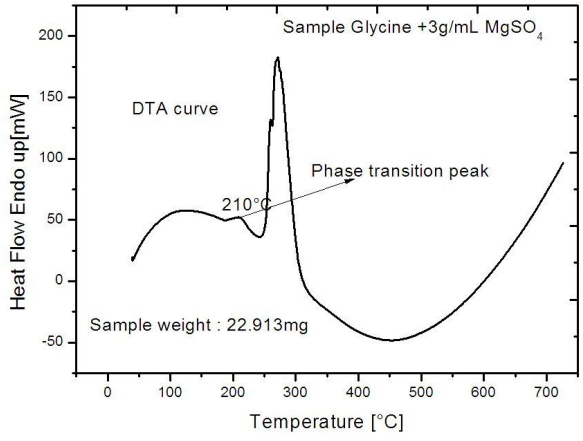

Fig. 15. Differential thermal thermogram (DTA) curve of γ-glycine crystal.

material is computed as a function of temperature while the substance and reference material are subjected to a controlled temperature program [36]. Differential scanning calorimetry thermograms of powdered glycine sample of α- and γ-polymorphs prepared at 1 g/mL to 3 g/mL of magnesium sulfate $MgSO_4$, respectively were recorded between 30 °C and 300 °C under nitrogen atmosphere using Mettler Toledo DSC 822e instrument. Fig. 16 and Fig. 17 show the DSC thermograms of α- and γ-polymorphs of glycine for polymorphic studies. The DSC thermograms of α- and γ-polymorphs of glycine illustrate that there is no physical water adsorption on the crystal molecular structure. The irreversible endothermic peak observed in DSC trace of α-glycine sample descends sharply at 255.32 °C which corresponds to the melting point of the sample whereas the DSC trace of γ-glycine sample exhibits a minor endothermic peak around 210 °C before the melting point of the sample. The minor peak around 210 °C is attributed to phase transformation from γ- to α-phase. The observed phase transition peak in DSC trace of γ-glycine sample increases more than that reported already by other researchers [29, 36].

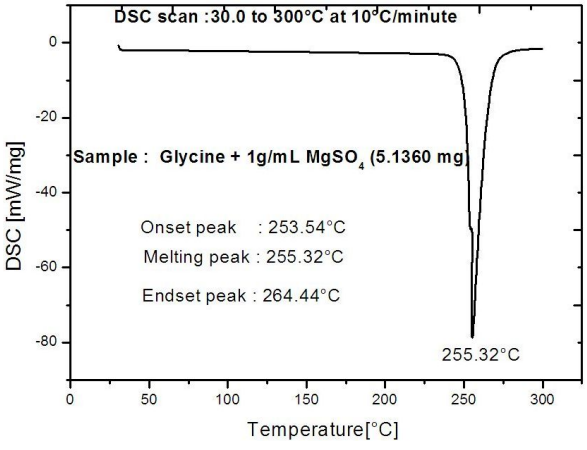

Fig. 16. DSC thermogram of α-glycine crystal.

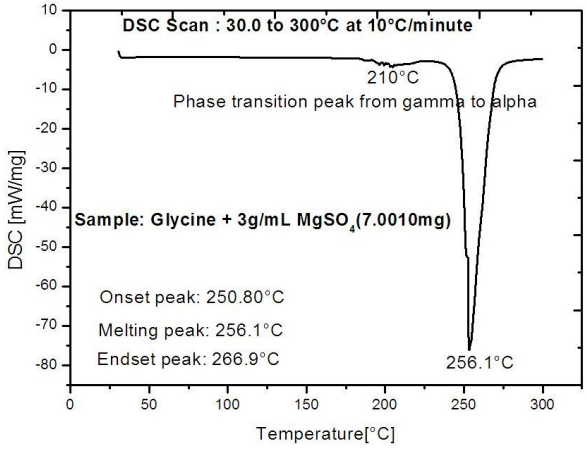

Fig. 17. DSC thermogram of γ-glycine crystal.

3.8. Optical UV-Vis-NIR transmittance analysis and photoluminescence (PL) study

The principle of ultraviolet-visible absorption is based on the phenomenon that molecules

holding π electrons or non-bonding electrons can absorb energy in the form of ultraviolet or visible light to excite these electrons to higher anti-bonding molecular orbitals, which leads to transitions among various electronic energy levels of the molecule. This procedure is used for characterizing the optical and electronic properties of various materials such as crystals, films and powders [15, 16]. The transmittance range recorded between 200 nm and 800 nm on crystals gives important information for its suitability in blue/green light applications. To exploit the usefulness of γ-glycine crystal for optical and other NLO applications, transmission range, cut-off wavelength and the energy bandgap were determined using Varian Cary 5000 UV-Vis-NIR spectrophotometer in the wavelength range of 200 nm to 800 nm. The obtained optical transmittance spectrum of γ-glycine crystal is depicted in Fig. 18. The percentage of optical transmittance between 200 nm and 400 nm was found to be 86 %. Also a lower cut-off wavelength, $\lambda_c = 200$ nm, than that observed in the transmittance spectrum was obtained. The transmittance spectrum of γ-glycine crystal reveals the existence of wide transparency window between the wavelength of 200 nm and 800 nm, low absorption in the entire UV-Vis region, higher percentage of transmittance value 89 % between wavelength 500 nm and 700 nm what suggests its suitability for optoelectronic, NLO, window materials in optical instruments, second harmonic generation and parametric oscillations applications. The energy bandgap E_g of the grown γ-glycine crystal was evaluated from Tauc plot of $(\alpha h\upsilon)^2$ versus photon energy [eV], as shown in Fig. 19 and its value was estimated from the intersection of extrapolated linear portion of $(\alpha h\upsilon)^2$ versus photon energy plot with x-axis. The obtained energy bandgap value is 5.83 eV showing dielectric nature of the crystal [14]. The photoluminescence emission behavior of γ-glycine single crystal grown from solution containing magnesium sulfate was studied and recorded by JASCO spectrofluorometer (model FP8300) in the range of 270 nm to 480 nm with an interval of 0.5 nm. The emission intensity of the PL spectrum is maximum at 311 nm (corresponding to energy of 3.98 eV, i.e. in near-violet region) as depicted in Fig. 20. Thus, the grown gamma glycine single crystal emits violet light suitable for photonics and optoelectronics applications.

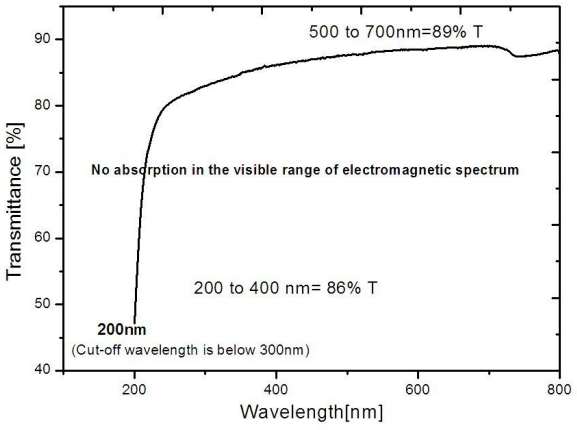

Fig. 18. UV-Vis optical transmittance spectrum of γ-glycine crystal.

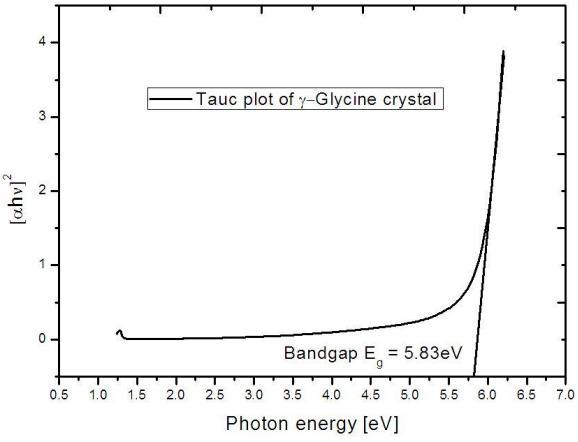

Fig. 19. Tauc plot of $(\alpha h\upsilon)^2$ versus photon energy (eV).

3.9. Vickers microhardness studies

Mechanical strength of trigonal pyramid shaped γ-glycine crystal grown from solution containing 3 g/100 mL $MgSO_4$ was studied by Vickers microhardness indenter at the applied loads of 25 g, 50 g, 100 g and 200 g. Hardness studies play an important role in device fabrication [39]. Vickers microhardness indenter has made several indentations at different positions on the crystal surface and the average value of diagonal length was taken as the

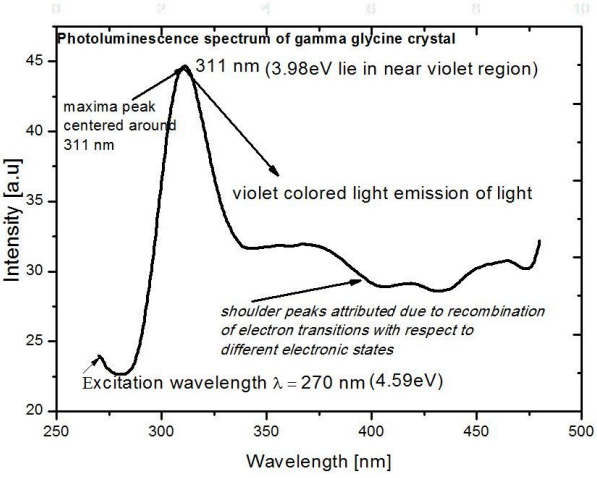

Fig. 20. PL spectrum of gamma glycine crystal.

Vickers hardness number H_v. The relation used for calculating microhardness was

$$H_v = 1.8544P/d^2[kg/mm^2] \quad (1)$$

where P is the applied load in g and d is the diagonal length of the indentation impression in μm. Fig. 21 shows the plot between the hardness number H_v and the applied load. It is observed from the graph that the Vickers hardness number H_v increases with applied load P. This type of behavior is due to Reverse Indentation Size Effect (RISE). The strength of materials can be understood by computing the work hardening coefficient n. The work hardening coefficient n, according to Onitsch et al. [39], should be less than 1.6 for hard materials and greater than 1.6 for soft materials. Fig. 22 presents a plot between logd and logP which is a straight line being in agreement with Meyer law. The work hardening coefficient or Meyer index number n was computed from the slope of the logd versus logP and it was found to be 3.44 which means that the grown γ-glycine crystal belongs to soft materials. The Vickers hardness number H_v was computed as 30.40 kg/mm^2 for 100 g load. The obtained hardness number H_v value (for 100 g load) is lower than that reported by Anbuchezhiyan et al. [29]. When the applied load P (in g) was increased above 100 g load, a microcrack was observed in the crystal due to the release of internal stress caused by indentation effect [39]. The yield strength of the grown gamma glycine single crystal was calculated from the relation

$$\sigma_y = (H_v/3)(0.1)^{n-2} \quad (2)$$

where H_v is Vickers hardness number, σ_y is the yield strength and n is Meyer index number or work hardening coefficient and the obtained yield strength value is 3.641 MPa. The grown gamma glycine single crystal has very low mechanical strength when it is compared with the literature data [29]. This may be due to the incorporation of magnesium sulfate into the crystal. The mechanical constants such as yield strength σ_y, elastic stiffness constant C_{11}, average crack length l, fracture toughness K_c, c/a ratio, brittleness index B_i, tensile strength T and yield point Y were computed and are presented in Tables 3 and 4. The computed mechanical parameters were compared with literature [41] and collected in Table 5.

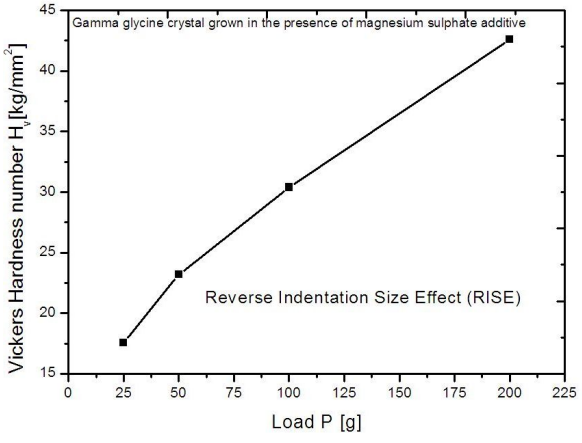

Fig. 21. Profile of Vickers hardness number versus load P.

3.10. Second harmonic generation verification test

The twinned trigonal pyramid shaped γ-glycine crystal grown from the solution containing 9 g/100 mL $MgSO_4$ was crushed, finely powdered using a mortar and pestle and it was densely packed in a microcapillary tube which was exposed normally to Q switched high energy Nd:YAG laser capable of producing input laser light beam of

Table 3. Computed mechanical parameters of γ-glycine crystal.

P Load [g]	Avg. value of Vickers hardness number H_v [kg/mm^2]	Diagonal length d [μm]	Yield strength σ_y=H_v/3(0.1)$^{n-2}$ [MPa]	Elastic stiffness constant C_{11}=$H_v^{7/4}$ [10^{14} Pa]	Avg. crack length ' l' [μm]	Fracture toughness K_c=P/$\beta_o l^{3/2}$ if l ⩾ d/2 where β_o=7 indentor constant [MNm$^{-3/2}$]	Ratio c/a (i) if c/a>2.5, crack is palmquist (ii) if c/a < 2.5, crack is a median or half penny	Brittleness index B_i $B_i = H_v/K_c$ [m$^{-1/2}$]
25	17.55	51.38	2.101	2.585		–		
50	23.20	63.11	2.779	4.213	81.03	–	1.7373	1087.85
100	30.40	78.57	3.641	6.762		–	Half penny crack	
200	42.60	93.28	5.103	12.205		0.384		

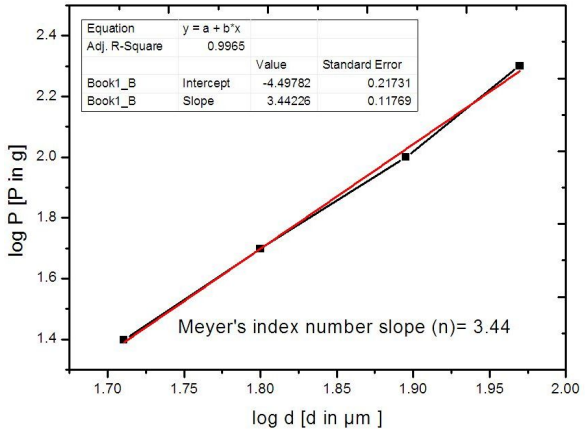

Fig. 22. Profile of logP versus logd.

Table 4. Computed tensile strength and yield point of the grown γ-glycine crystal.

Vickers hardness number H_v [MPa]	Tensile strength $T = 0.2\ H_v + 6$ [MPa]	Yield point $Y = 0.23H_v - 13.5$ [MPa]
172.09	40.4	26.0
227.49	51.4	38.8
298.10	65.6	55.0
417.73	89.5	82.5

1064 nm with the pulse width of 8 ns at a repetition rate of 10 Hz. The bright green light emission (λ = 532 m) from the powdered crystalline sample of γ-glycine confirmed the frequency-doubling character and non-centrosymmetric packing of γ-glycine crystal structure. The input energy 0.689 J was passed through powdered crystalline samples of γ-glycine and a reference material KDP. The obtained output energy of powdered γ-glycine sample was 11.25 mJ whereas the reference material KDP gave 7.80 mJ. The computed SHG efficiency of γ-glycine crystal grown in the presence of $MgSO_4$ additive is 1.44 times greater than that of potassium dihydrogen orthophosphate KDP. Further, it is interesting to note that the SHG efficiency is augmented from 1.31 to 1.44 as the concentration of $MgSO_4$ additive increased from 3 g/mL to 9 g/mL.

4. Conclusions

The performed slow solvent evaporation crystallization experiments explain the growth mechanism and crystal habit of α and γ polymorphs of glycine grown in the presence of different concentrations of magnesium sulfate salt viz. 0.1 g/mL to 16 g/mL. Addition of lower concentration of magnesium sulfate (0.1 g/mL to 0.5 g/mL) into glycine saturated solutions showed usual morphology of α-form (i.e. crystal length c > a) whereas the concentration of magnesium sulfate in the range of 0.5 g/mL to 1.5 g/mL yielded different morphology than typical morphology of α-form (i.e. crystal length a > c). This habit trend has changed suddenly when the critical concentration of magnesium sulfate reached 2 g/mL. The resulting

Table 5. Comparison of mechanical constants with literature data.

Mechanical constant	Present work	Literature [41]
Fracture toughness K_c [$MNm^{-3/2}$]	0.3840	0.6952
Ratio c/a	1.7373	2.09
Nature of crack	Half penny crack or median crack	Half penny crack or median crack
Brittleness index B_i [$m^{-1/2}$]	1087.85	470.911
Meyer's number n	3.44	4.8
Material category	Very soft material	Soft material
Additive used in glycine aqueous solutions	Magnesium sulfate	Sodium bromide

crystals have trigonal pyramid shaped smooth facets and truncated tip at one end of the top +c-axis and rough pyramid shaped non-crystallographic facets at the opposite end of bottom –c axis. In addition, to trigonal pyramid shaped habit, twinned trigonal shaped morphology and multiple twinned clusters of trigonal pyramid shaped morphology were noticed in the crystal growth experiments at higher concentrations of magnesium sulfate salt. The unidirectional growth behavior of γ-glycine crystal was obtained at 3 g/100 mL concentration of $MgSO_4$. The samples were subjected to SXRD, PXRD, NMR, FT-IR, ICP-OES, TG-DTG-DTA, DSC, UV-Vis-NIR, microhardness and SHG characterization studies. Single crystal XRD and powder XRD studies revealed that the grown crystal is γ-glycine with non-centrosymmetric space group $P3_2$ crystallized in hexagonal crystal system. The lattice parameters and unit cell volume were computed from powder XRD data using unit cell software program. Elemental analysis ICP-OES allowed us to assess the concentration of magnesium element present in the glycine samples. The incorporation of additive element magnesium into the crystalline matrix of γ-glycine was confirmed by ICP-OES, proton ^1H and carbon ^{13}C NMR spectra and FT-IR studies. Fourier transform infrared spectroscopic spectra analysis displayed the fingerprint distinction between α- and γ-polymorphs of glycine. Thermal parameters: decomposition point or melting point, weight loss and γ- to α-glycine phase transition were clearly explained by TG-DTA thermograms. The γ- to α-glycine phase transition at 210 °C was confirmed both by TG-DTA and DSC thermograms. The low cut-off wavelength (200 nm) combined with good transmittance (86 %) in the UV-Vis region indicates that the grown γ-glycine crystal may be used in optoelectronic, SHG harmonic generation and photonics applications. The photoluminescence spectrum examination on the grown gamma glycine crystal revealed prominent violet colored emission of light from the crystal. Mechanical parameters such as mechanical strength, Vickers hardness number, Meyer index number and yield strength of the γ-glycine crystal were calculated. The grown γ-glycine crystal belongs to soft category. Second harmonic generation Kurtz powder nonlinear optical test [40] confirmed the existence of frequency doubling in γ- glycine crystal and its SHG efficiency was calculated as 1.44 times superior than that of KDP material.

References

[1] CABRERA N., VERMILYEA D.A., *The Growth of Crystal from Solution.* in:DOREMUS R.H., ROBERTS D.B.W., TURNBULL (Eds.), *Growth and Perfection of Crystal,* Chapman & Hall London, 1958.
[2] LITAKA Y., *Acta Crystallogr.,* 14 (1961), 1.
[3] LITAKA Y., *Acta Crystallogr.,* 11 (1958), 225.
[4] LITAKA Y., *Proc. Jpn. Acad.,* 30 (1954), 109.
[5] LITAKA Y., *Acta Crystallogr.,* 13 (1960), 35.
[6] SENDHIL. K. POORNACHARY., PUI SHAN CHOW., REGINALD B.H.TAN., *J. Cryst. Growth,* 310 (2008), 3034.
[7] SENDHIL. K. POORNACHARY., PUI SHAN CHOW., REGINALD B.H.TAN., *Cryst. Growth Des.,* 8 (2008), 179.
[8] DAWSON A., ALLAN D.R., BELMONTE S.A., CLARK S.J., DAVID W.I.F., MC GREGOR P.A., PARSONS S., PULHAM C.R., SAWYER L., *Cryst. Growth Des.,* 5 (2005), 1415.

[9] MARSH R.E., *Acta Crystallogr.,* 11 (1958), 654.
[10] BOLDYREVA E.V., *Crys. Eng*., 6 (2003), 235.
[11] NARAYAN BHAT M., DHARMAPRAKASH S.M., *J. Cryst. Growth,* (2002) 242.
[12] NARAYANA MOOLYA B., JAYARAMA A., SURESHKUMAR M.R., DHARMAPRAKASH S.M., *J.Cryst.Growth,* 280 (2005), 581.
[13] DILLIP G.R., RAGHAVAIAH P., MALLIKARJUNA K., MADHUKAR REDDY C., BHAGAVANNARAYANA G., RAMESH KUMAR V., DEVA PRASAD RAJU B., *Spectrochim. Acta Part A,* 79 (2011), 1123.
[14] ZULIFIQAR ALI AHAMED S.D., DILLIP G.R., RAGHAVAIAH P., MALLIKARJUNA K., DEVA PRASAD RAJU B., *Arab. J. Chem.,* 6 (2013), 429.
[15] DILLIP G.R., BHAGAVANNARAYANA G., RAGHAVAIAH P., DEVA PRASAD RAJU B., *Mater. Chem. Phys.,* 134 (2012), 371.
[16] PARIMALADEVI R., SEKAR C., *Spectrochim. Acta Part A*, 76 (2010), 490.
[17] ANBUCHUDAR AZHAGAN S., GANESAN S., *Optik,* 11 (2012), 993.
[18] ANBUCHUDAR AZHAGAN S., GANESAN S., *Optik,* 6 (2013), 526.
[19] ANBUCHUDAR AZHAGAN S., GANESAN S., *Optik,* 15 (2013), 2251.
[20] ANBU CHUDAR AZHAGAN S., GANESAN S., *Optik,* 20 (2013), 4452.
[21] ANBU CHUDAR AZHAGAN S., GANESAN S., *Optik*, 23 (2013), 6456
[22] ANBUCHUDAR AZHAGAN S., GANESAN S., *IJPS,* 8 (2013), 6.
[23] ANBU CHUDAR AZHAGAN S., GANESAN S., *Arab. J. Chem.,* 10 (2017), S2615.
[24] SRINIVASAN K., RENUGA DEVI K., ANBUCHUDAR AZHAGAN S., *Cryst. Res. Technol.,* 46 (2011), 159.
[25] SRINIVASAN K., *J. Cryst. Growth*, 311 (2008), 156.
[26] SRINIVASAN K., ARUMUGAM J., *Opt. Mater.,* 30 (2007), 40
[27] RENUGA DEVI K., SRINIVASAN K., *Cryst. Res. Technol.,* 50 (2015), 389.
[28] BALAKRISHNAN T., RAMESH BABU R., RAMAMURTHI K., *Spectrochim. Acta Part A*, 69 (2008), 1114.
[29] ANBUCHEZHIYAN M., PONNUSAMY S., SINGH S. P., PAL P.K., DATTA P.K., MUTHAMIZHCHELVAN C., *Cryst. Res. Technol.*, 45 (2010), 497.
[30] YOGAMBAL C., EZHIL VIZHI R., RAJAN BABU D., *Cryst. Res. Technol.*, 50 (2015), 22.
[31] SEKAR C., PARIMALADEVI R., *Spectrochim. Acta Part A,* 74 (2009), 1160.
[32] *Organic Index to the Powder Diffraction File, Joint committee of Powder Diffraction Standards*, 2002.
[33] GUANGWEN HE., VENKATESWARLU BHAMIDI., SCOTT. R. WILSON., REGINALD B.H.TAN., PAUL J.A. KENIS., CHARLES F.ZUKOSKI., *Cryst. Growth Des.,* 6 (2006), 1746.
[34] TOWLER C.S., DAVEY R.J., LANCASTER R.W., PRICE C.J., *J. Am. Chem. Soc.,* 126 (2004), 13347.
[35] LI L., LECHUGA-BALLESTEROS D., SZKUDLAREK B.A., NAIR RODRIGUEZ- HORNEDO N., *J. Colloid. Interf. Sci.,* 168 (1994), 8.
[36] PERLOVICH G.L., HANSEN L.K., BAUER-BRANDL A., *J. Therm. Anal. Calorim.,* 66 (2001), 699.
[37] SILVERSTEIN R., BASSLER G.C., MORRILL T.C., *Spectrometric Identification of Organic compounds,* John Wiley & Sons, New York, 1981.
[38] BRUICE P.Y., *Organic chemistry,* Pearson Education Pvt. Ltd., New Delhi, 2002.
[39] ONITSCH E.M., *Mikroskopie,* 95 (1956), 2.
[40] KURTZ S.K., PERRY T.T., *J. Appl. Phys.,* 39, (1968), 3798.
[41] EZHIL VIZHI R., YOGAMBAL C., *J. Cryst. Growth,* 452 (2016), 198.

Received 2018-08-20
Accepted 2019-03-16